



HAL
open science

Optical method for evaluation of shrinkage in two dimensions during drying of ceramic green bodies

Siham Oummadi, Benoit Nait-Ali, Arnaud Alzina, Marie-Clotilde Paya,
Jean-Marie Gaillard, David Smith

► **To cite this version:**

Siham Oummadi, Benoit Nait-Ali, Arnaud Alzina, Marie-Clotilde Paya, Jean-Marie Gaillard, et al..
Optical method for evaluation of shrinkage in two dimensions during drying of ceramic green bodies.
Open Ceramics, 2020, 2, pp.100016. 10.1016/j.oceram.2020.100016 . hal-03407006

HAL Id: hal-03407006

<https://unilim.hal.science/hal-03407006v1>

Submitted on 5 Sep 2022

HAL is a multi-disciplinary open access archive for the deposit and dissemination of scientific research documents, whether they are published or not. The documents may come from teaching and research institutions in France or abroad, or from public or private research centers.

L'archive ouverte pluridisciplinaire **HAL**, est destinée au dépôt et à la diffusion de documents scientifiques de niveau recherche, publiés ou non, émanant des établissements d'enseignement et de recherche français ou étrangers, des laboratoires publics ou privés.



Distributed under a Creative Commons Attribution - NonCommercial 4.0 International License

Optical method for evaluation of shrinkage in two dimensions during drying of ceramic green bodies

Siham OUMMADI, Benoit NAIT-ALI*, Arnaud ALZINA, Marie-Clotilde PAYA,
Jean-Marie GAILLARD, David S. SMITH

University of Limoges, IRCER , UMR CNRS 7315, 12 rue Atlantis, F-87068 Limoges, France.

Abstract

The evolution of shrinkage and mass during drying of kaolin and alumina green bodies was characterized. Standard practise uses a position sensor with simultaneous mass measurement. In this work an optical method was developed to follow shrinkage in two orthogonal directions. Green body samples were made by pressing of ceramic pastes. Results have been compared through the well known Bigot curves which show two distinct stages. First a linear shrinkage with the evaporated water loss is observed. Then in the second stage with further water loss, negligible dimension changes occur. For each material, the overall shrinkage values are identical in the two directions parallel to the pressing axis, but higher in the pressing direction. This difference is related to the shaping method yielding a preferential orientation of grains. Anisotropy in shrinkage is more significant for kaolin with tabular shaped grains compared to the more isometric grains of alumina.

Keywords: Drying; Shrinkage; Anisotropy

1. Introduction

Ceramic materials are often prepared using shaping methods which involve incorporation of water. Drying is then a necessary step before final firing is made to achieve a robust ceramic. In the complete process of fabrication, drying and firing are two steps which result in body shrinkage, determining the final dimensions of a ceramic object. Drying shrinkage,

*Corresponding author: benoit.nait-ali@unilim.fr

not only, results in dimensional change but also internal stresses. These can be a source of damage in the object if they become too strong. Obviously a well mastered processing route with careful control of the powder granulometry and forming method seeks to avoid such a situation. Another issue related to drying is the energy consumption required to evaporate water. This is particularly significant for traditional ceramic industries such as tile, brick and tableware manufacture, involving high volume production. Industrially, the objectives are to minimize the energy and time expended, maintain dimensional control of the final ceramic object and avoid the presence of defects such as cracks [1, 2, 3]. Investigation of the drying behaviour of a ceramic paste is then of strong importance. A popular and much used method of investigating the behaviour of a ceramic paste consists of monitoring the length and mass during slow drying in constant conditions to ensure a uniform shrinkage. Removing the time dependence by plotting the water content as a function of the linear shrinkage gives the well-known Bigot curve [4, 5]. This method of examining the drying behaviour of ceramic green bodies with a representation of the linear shrinkage and the water content in the same graph was also proposed by Kingery [6]. Kornmann has reviewed the Bigot curve and summarized the important information which can be extracted from the curve as well as discussing the limitations to the interpretation [7]. The key point is identification of the water content below which the shrinkage becomes negligible. This is known as the critical moisture content. Before the critical moisture content is attained, drying has to be performed carefully to avoid defects due to shrinkage. Bigot curves are used today to study drying behaviour which can vary depending on raw materials, component proportions in the paste mixture, additives or drying conditions [8, 9, 10, 11].

In the field of mechanics, methods have been developed to measure displacement or strain field of a surface from digital images obtained using optical cameras. For example methods based on tracking of marks or on digital image correlation have been reported [12]. Optical cameras have already been used to investigate drying of ceramics, for example to study crack formation in clay materials or to determine shrinkage in concrete samples [13, 14]. In this work we present a new approach for determining Bigot curves in two directions simultaneously

with a view to investigating materials with possible anisotropic shrinkage as in the case of clays. We have used optical cameras to monitor the displacements simultaneously with weight loss in order to plot the Bigot curves. Two ceramic materials, characterized by significantly different grain shapes, were studied: alumina and a kaolin clay. Results are compared with curves obtained with a position sensor operating in one dimension. They are discussed in relation to the microstructures of the ceramic materials.

2. Materials and methods

2.1. samples preparation

The first raw material was an α -alumina powder, denoted P172SB, supplied by Alcan. This has a small grain size, represented by a median size of $0.4 \mu\text{m}$ and a specific surface area of $7.5 \text{ m}^2\text{g}^{-1}$. The alumina powder was chosen for its frequent use in technical ceramic products. The second raw material was a kaolin powder, called BIP kaolin, supplied by Imerys Ceramic France after extraction from the Beauvoir site. This raw material is a clay powder used in traditional ceramic products. Its specific surface area is about $10 \text{ m}^2\text{g}^{-1}$, and the median grain size measured using laser light scattering (Malvern Master-sizer 2000) is $9.5 \mu\text{m}$. The high value of grain size for this kaolin powder compared to the specific surface area suggests that the grains are agglomerated.

In order to obtain a homogeneous slurry, each powder was mixed with water and stirred in a jar for 75 min according to the mass quantities in the first column of Table 1. Then the slurries were cast on a plasterboard to absorb a part of the initial water yielding a homogeneous ceramic paste which can be handled. The water content in the pastes are given in the second column of Table 1. Even if the mass percent of water is different in the two pastes, the volume percent of water is approximately the same (55% for alumina and 53% for kaolin). To avoid premature evaporation before the drying study, the paste was covered with a plastic film and placed in a chamber saturated with water vapor. Before each measurement, a portion of the paste was extracted and pressed in one direction. Then the samples were cut using a thin metallic wire with the dimensions of $20 \text{ mm} \times 20 \text{ mm} \times 7 \text{ mm}$ as illustrated

in Fig. 1.

| | mass% DB | mass% WB | vol.% |
|--------------------|----------|----------|-------|
| Alumina suspension | 100 | 50 | 80 |
| Kaolin suspension | 186 | 65 | 83 |
| Alumina paste | 31 | 24 | 55 |
| Kaolin paste | 44 | 31 | 53 |

Table 1: Water contents in the initial suspensions and in the pastes. Calculated in mass% on a dry basis (DB), mass% on a wet basis (WB) and in vol.% of the total volume.

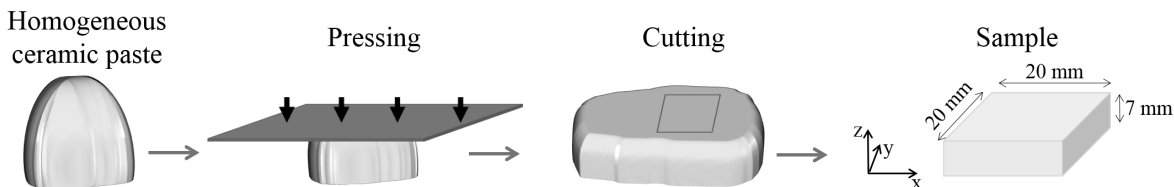


Figure 1: Schematic description of the different steps of sample preparation.

2.2. Water content and shrinkage measurements

Monitoring the variation of sample dimensions in different directions simultaneously with the weight loss as a function of time was performed using two different methods. For all measurements, the drying of samples was evaluated in similar conditions, i.e. at room temperature (20 °C), and ambient relative humidity with the same surface exposed to drying. **These drying conditions ensure a slow drying and the recording time was 24 hours.**

2.2.1. 1D measurement

In the first method the dimension variation was followed in one direction. The sample weight was monitored using a BC220M Precisa balance which has a sensitivity of 1 mg. The height of the sample was measured using a Linear Variable Differential Transformer (LVDT) sensor which has a measuring range of 6 mm and a resolution of $\pm 5 \mu m$. The experimental set-up is illustrated in Fig. 2. With this equipment, three experiments were performed with different sample orientations, to obtain shrinkage in three orthogonal directions.

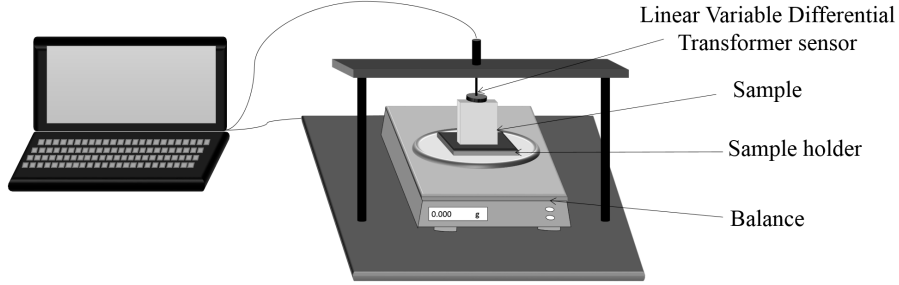


Figure 2: Schematic representation of the experimental setup for shrinkage measurement in 1D.

2.2.2. 2D measurement: optical method

In this second method the measurements were performed with the use of the same balance, and a uEye SE camera supplied by IDS with a resolution of $2590 \text{ pixels} \times 1920 \text{ pixels}$. With this method, variations of sample dimensions were identified simultaneously in two directions during drying. Schematic representation of the experimental set-up is given in Fig. 3(a). The sample was placed on a support which was lubricated with oil to avoid mechanical stresses resulting from adhesion with the support during drying. Each material, alumina and kaolin, was measured with two different sample orientations in order to monitor the variation of dimensions in three directions. Several colored full circles were marked on the sample surface before starting the measurement as shown in Fig. 3(b). Then the images and the sample weight were recorded every 5 minutes.

In order to accurately determine the sample dimension changes in two directions, the distances between the full circles of images were evaluated with the use of a program written in Python. Image analysis typically involves different steps. The first step corresponds to cropping of images in order to focus the analysis on the sample surface as illustrated in Fig. 4(a and b). Then as the images were taken at different times during drying and the sample state changes with water removal, the lighting conditions were not the same. For that reason, a specific adaptable threshold was used. Then a blur function was applied to the images in order to detect the full circle contours and their centers (Fig. 4(c and d)). Based on the distance values between the pairs of the full circles for each image during drying $L(t)$ and those of the last image which corresponds to the dry sample L_d , the shrinkage (S) in two

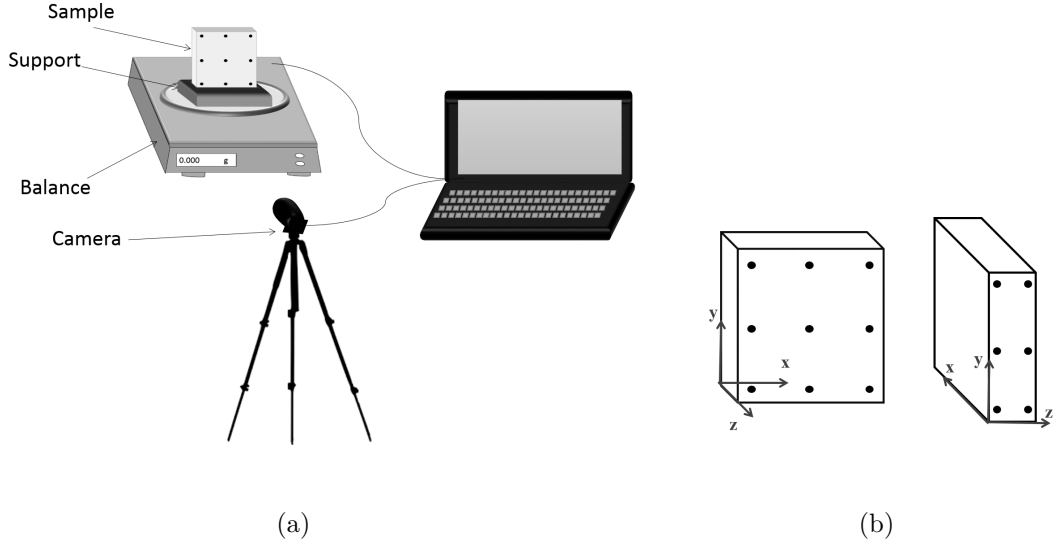


Figure 3: a) Experimental setup for shrinkage measurement in 2D. b) Two experiments to measure shrinkage in all directions (with full circles on the observed face).

orthogonal directions was calculated using the relation:

$$S = \frac{L(t) - L_d}{L_d} \quad (1)$$

For each direction, the shrinkage was evaluated by taking an average value over all the pairs of full circles. Furthermore, since the sample shrinkage is in three orthogonal directions, the resolution of the pixels per unit length number changes slightly. A correction was made to take this effect into account.

According to the obtained sample mass m , the water content W was calculated with the relation:

$$W = \frac{m(t) - m_d}{m_d} \quad (2)$$

where m_d is the mass after drying at 110 °C until a constant value is achieved.

2.3. Microstructure observations

A Scanning Electron Microscope (SEM), type FEI Quanta 450 FEG, was used to observe the microstructure of the samples. Before the observations, samples were dried in an oven at

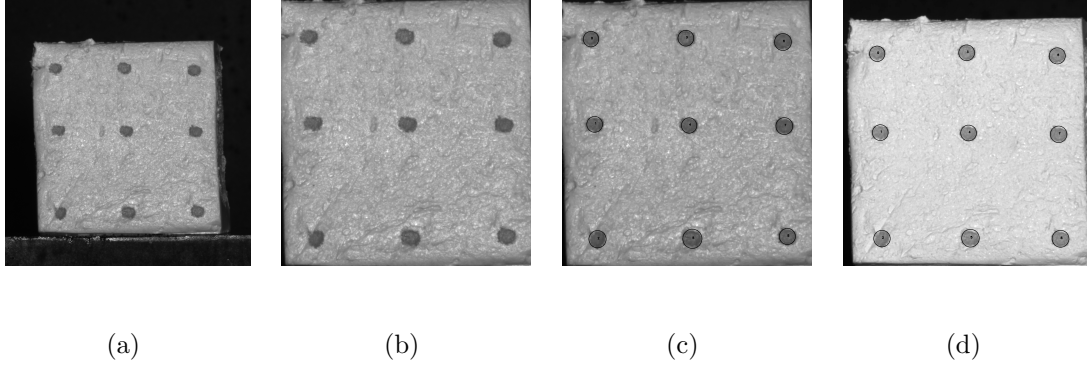


Figure 4: Representation of the different steps of image analysis for square shaped samples of kaolin. a) Raw image. b) Image cropped to the sample surface. c) Contour detection at the beginning of drying. d) Contour detection at the end of drying.

110 °C for 24 hours to ensure complete water removal. Then they were fractured in order to observe two cuts: the perpendicular and the parallel cuts to the pressing direction.

3. Results and discussion

3.1. Bigot curve description

Bigot proposed in 1921 to plot the water content on a dry basis as a function of linear shrinkage on a wet basis [4]. These graphs were useful for the study of drying but with the inconvenience that, for a given powder, the description requires a set of curves each with a different initial water content. Munier then suggested to plot water content and linear shrinkage both on a dry basis to obtain a single curve describing the behaviour during drying [5]. Referred to as the Bigot curve, a typical example is shown in Fig. 5. At the beginning of drying, grains are not in contact but separated by a thin film of water, giving plasticity to the paste. During the major shrinkage stage, the volume of water which is evaporated results in a volumetric shrinkage. This corresponds essentially to the linear part of the curve. At point PL, which is defined as the plasticity limit, grains start to make contact. A transition then occurs to a stage where grains are fully in contact and shrinkage becomes negligible despite further water loss. Based on this description of the behaviour, the Bigot curve is then used to determine:

- the overall shrinkage,
- the amount of water which fills the pores, assuming grains are in contact, called Interstitial Water (IW),
- the additional amount of water which separates grains, sometimes called colloidal water (because colloidal clay particles become separated). The transition from evaporation of colloidal water to removal of interstitial water corresponds to the critical point in the drying process. Before this point is attained, conditions of temperature, humidity and air flow should be set for slow drying in order to avoid deformation of the ceramic body or formation of cracks.

For the study of transformations in particulate systems during ceramic processing, Onoda proposed a related description of the system by plotting the specific volume (inverse density) as a function of water mass fraction. The resulting graph is called a specific volume diagram in which the same stages as shown in Fig. 5 can be distinguished [15, 16].

Assuming that the paste is initially free of pores, the interstitial water amount W_{IW} , which is defined as the intercept with the y-axis in the Bigot curve can be related to the volume fraction of the pores (p) in the dried samples:

$$W_{IW} = \frac{p\rho_w}{(1-p)\rho_s} \quad (3)$$

where ρ_w and ρ_s are respectively the density of water and the solid phase. The portion of the curve corresponding to the major shrinkage can be expressed by the relation, assuming an isotropic shrinkage:

$$W = \frac{\rho_w[(S+1)^3 - 1 + p]}{(1-p)\rho_s} \quad (4)$$

For small values of shrinkage, this expression can be simplified leading to a linear behaviour:

$$W = \frac{\rho_w(3S+p)}{(1-p)\rho_s} \quad (5)$$

However the behaviour is more complex if the shrinkage is anisotropic. This requires investigation in multiple directions and is related to the raw material characteristics (in particular the grain shape) and the forming method which can induce preferential orientation of grains.

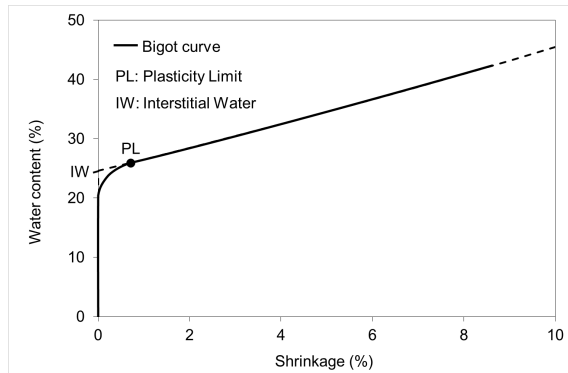


Figure 5: Example of a Bigot curve: water content as a function of shrinkage both on a dry basis. The point PL represents the plasticity limit when grains begin to be in contact. The dotted line can be plotted using Eq. (4) or Eq. (5) if pore volume fraction and solid phase density are known.

3.2. Alumina samples

The Bigot curves in x, y and z directions were established for drying of alumina samples using both methods which give very similar results in Fig. 6. It can be noted that from the beginning of drying, the shrinkage for each direction decreases linearly with water loss down to 24% of water content within the sample and then exhibits a negligible variation until the end of drying. Also based on Fig. 6, we can distinguish different amounts of shrinkage depending on directions. It is almost identical in x and y directions (ca. $\sim 4\%$) but increases in the z direction (ca. $\sim 5\%$) for both the LVDT and optical measurements. This difference in the overall shrinkage as a function of water content, corresponding to a factor of 1.2 between the z direction and the other directions, can be explained by the nature of the raw material and the sample preparation. In fact, pressing a paste of isometric grains should not yield any preferential orientation. Accordingly, shrinkage in the three orthogonal directions should be similar. This is not quite the case here, since alumina particles are not strictly isometric. Therefore, to investigate further the preferential orientation, we present in Fig. 7 two SEM images corresponding to cuts perpendicular (Fig. 7(a)) and parallel (Fig. 7(b)) to the pressing direction. The observations confirm that grains are not perfectly isometric and seem to be oriented as shown in Fig. 7(a) with larger surface area of grains compared to Fig. 7(b). This may explain a slight anisotropy in shrinkage for these alumina samples.

By rearranging Eq. (3), a value for the porosity p can be calculated corresponding to a value of interstitial water $W_{IW}=0.24$. This yields a porosity of 49% which is very close to the measured value ($48\% \pm 2\%$). The calculated curve, for isotropic behaviour, given by Eq. (4) is then plotted in Fig. 6(b) and lies between the experimental curves for the z and x,y directions. The calculated and experimental curves are consistent with similar volumetric shrinkages, here approximately 13%. Therefore, we confirm experimentally that the slope of the Bigot curve for isotropic shrinkage is determined by the ratio of the fluid to solid phase densities as well as the pore volume fraction of the dry green body. Furthermore, the curve can be used to deduce this last piece of information via the point IW. In the next section, kaolin clay exhibiting anisotropic shrinkage on drying is studied using the same approach.

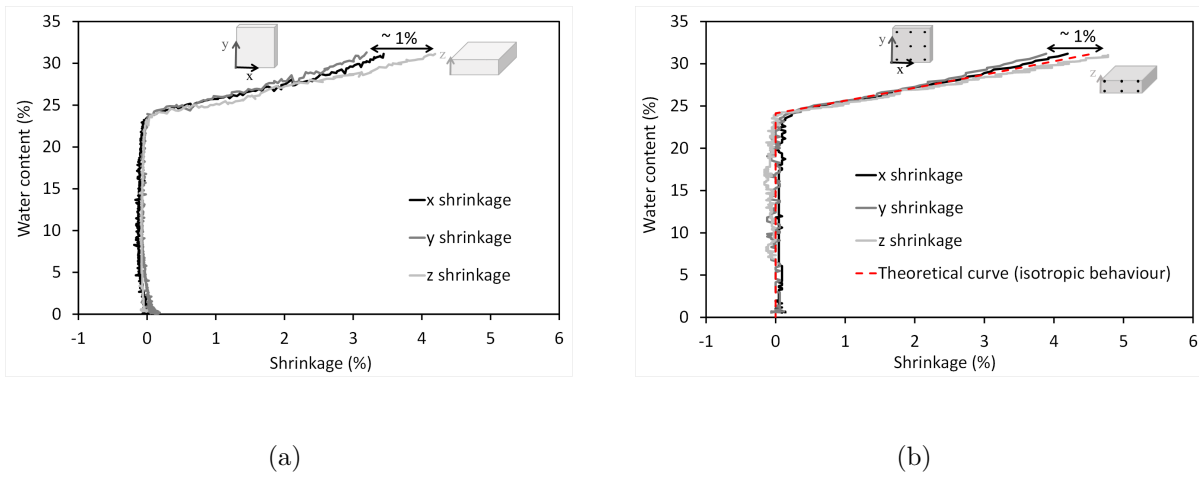


Figure 6: Bigot curves for alumina samples dried at room temperature and in conditions of ambient relative humidity for three orthogonal directions. a) Measured with the LVDT sensor. b) Measured with the camera.

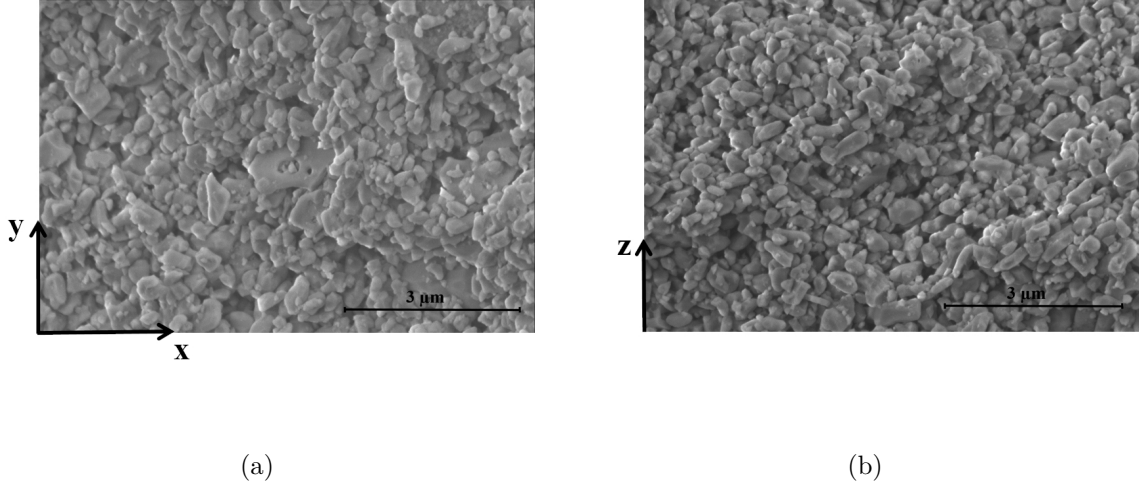


Figure 7: SEM micrographs on fractures of the alumina samples completely dried in at 110 °C. a) Observation of the perpendicular cut to the pressing axis. b) Observation of the parallel cut to the pressing axis.

3.3. kaolin samples

Bigot curves measured in three orthogonal directions for kaolin samples with the 1D and 2D methods are presented in Fig. 8. The experimental curves agree closely with both methods. Initially the water content within samples is the same (44%). Results show that the mass loss is linear with shrinkage until the water content reaches approximately 25%. Shrinkage becomes then negligible in the three directions simultaneously. The main difference compared to curves obtained for alumina samples is that variation in the overall shrinkage for the three directions yields a wider interval, between 6% and 11%. This corresponds to a factor of 1.8 between the z direction and the other two directions. Similar to alumina samples, greater shrinkage is observed in the z direction. Indeed, since the kaolin grains have a tabular form, we assume that a preferential orientation of grains due to pressing could correlate with the higher shrinkage value in the z direction.

In order to investigate further the preferential orientation of kaolin platelets due to the pressing step, we present two SEM images corresponding to cuts perpendicular (Fig. 9(a)) and parallel (Fig. 9(b)) to the pressing direction. In Fig. 9(a), tabular shaped grains can be observed without noticeable preferential orientation which is in accordance with similar shrinkage values measured in x and y directions. However, in Fig. 9(b), stacking of the kaolin

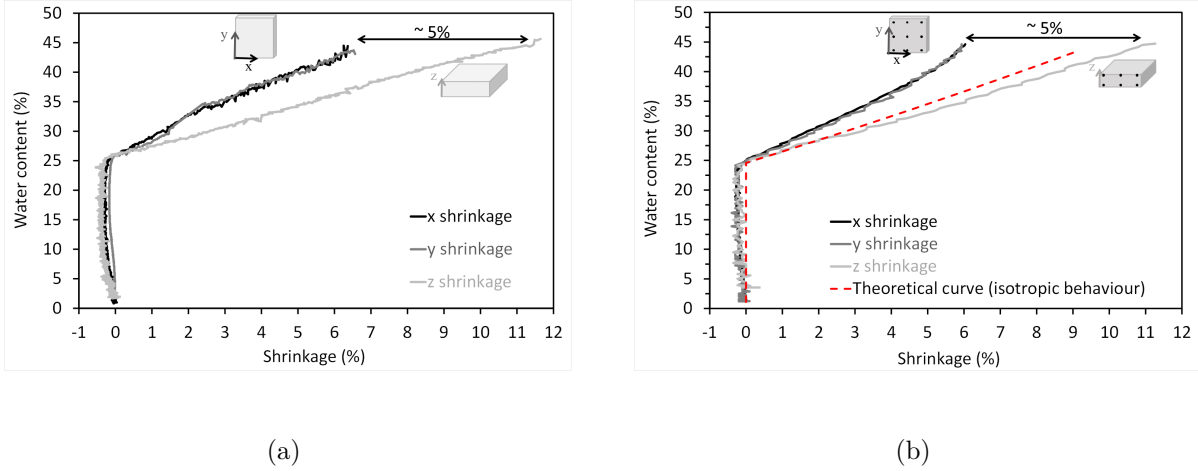


Figure 8: Bigot curves for kaolin samples dried at room temperature and in conditions of ambient relative humidity for three orthogonal directions. a) Measured with the LVDT sensor. b) Measured with the camera.

platelets along the z direction can be observed with basal planes oriented perpendicular to this direction. Based on these observations, the higher shrinkage revealed in z direction can then be explained by this preferential orientation with a higher number of grains/water interfaces per unit length in this particular direction. At the beginning of drying the platelets are surrounded by liquid water as illustrated in Fig. 10(a). Though the distribution of water in the green body is uniform in this first stage [17], the number of water layers per unit length is higher along z than in the other directions and consequently the removal of the water layers leads to greater shrinkage along z (Fig. 10(b)). Based on a grain size of $4 \mu\text{m}$ in x - y plane, a simple estimate of the starting water film thickness, in case of perfect orientation, is 200 nm. This is consistent with earlier work by Ford who discussed the anisotropy in shrinkage behaviour of clay materials, explaining that when the number of water films per unit length is different in the two directions, the shrinkage is also different [3]. In the real situation, the distribution of particle sizes and orientations should be taken into account.

The calculated curve, for an equivalent isotropic behaviour (Eq. (4)), is also plotted in Fig. 8(b). The porosity content corresponding to $W_{IW}=0.25$ is 39% which is very close to the measured value ($40\% \pm 2\%$). Again the calculated curve, with the assumption of isotropic shrinkage lies between the experimental curves for the z and x,y directions with a

volumetric shrinkage of approximately 25%. This plot illustrates clearly the deviations from isotropic behaviour (red line) of the kaolin sample during drying. Such differential shrinkage may be a source of incompatible stresses at the end of the constant rate period resulting in body deformation or damage. Thus, the approach with an optical camera has potential for qualitative identification of such situations in an industrial context.

It is now useful to set the approach and results of the study in a more general context. Analysis of the optical images for tracking of marks via a computer program is fairly straightforward. The displacements can be calculated with precision providing they are not too small. This is the particular case of the first stage of drying where shrinkage amounts are macroscopic (visible to the naked eye). In contrast, by the start of the second stage, the residual shrinkages obtained from optical images contain substantial noise. Results would be improved with the use of average values taken over short time intervals. However to gain significantly more accuracy techniques based on Digital Image Correlation (DIC) become of strong interest. These techniques, which are widely used in the study of mechanical properties of solids to obtain detailed information on local strain gradients, use a speckle pattern or a grid deposited on the body surface[18]. The speckle pattern must be of good quality in order that the different locations on the body surface can be followed as a function of time. For the study of a body made of ceramic paste the use of paint or spray for the speckle pattern will be complicated by any interactions with the drying process. Other techniques use a real or virtual grid network. In principle, the grid network coupled with heterogeneous loading, for example with localized air flows, could identify with a single trial the strain matrix associated with shrinkage. This approach based on the method of virtual fields has been demonstrated in the study of predominant thermal and mechanical behaviour of anisotropic composites [19]. In future work, localized strain information obtained by optical methods could also be exploited as valuable input data for a computer model of the drying ceramic body.

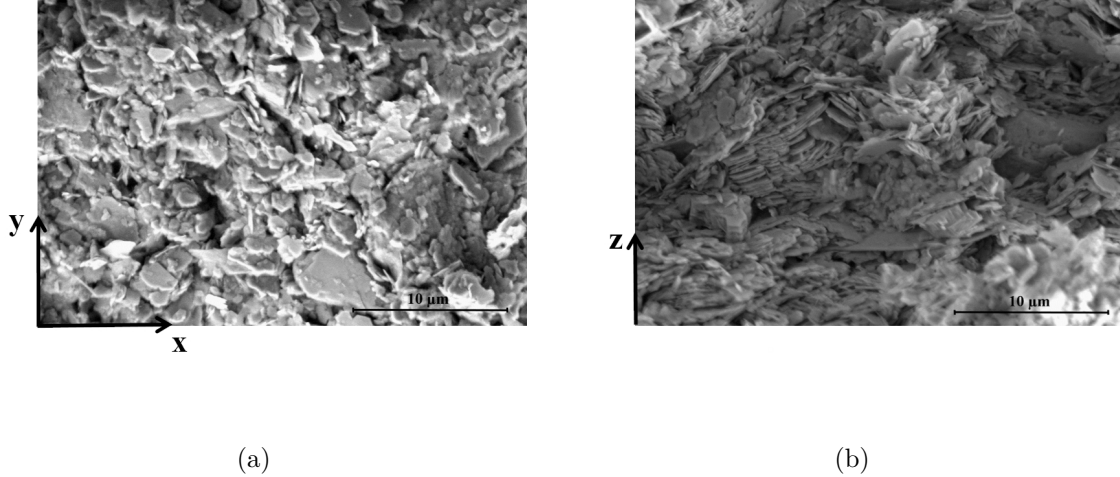


Figure 9: SEM micrographs on fractures of the kaolin samples previously dried at 110 °C. a) Observation of the perpendicular cut to the pressing axis. b) Observation of the parallel cut to the pressing axis.

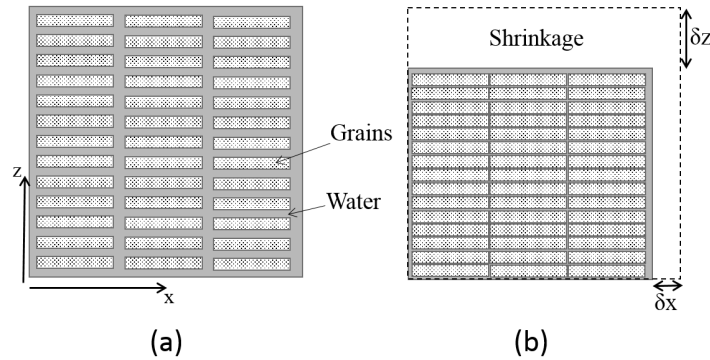


Figure 10: Schematic arrangement of grains with the same number of grains. a) At the beginning of drying. b) At the end of major shrinkage.

4. Conclusion

An optical method based on tracking of marks has been developed to measure linear shrinkage, simultaneously in two dimensions, during drying of ceramic pastes. To illustrate the interest of such a method in the field of ceramics, kaolin and alumina pastes were characterized. Results obtained with this method are found to be in good agreement with those obtained with a LVDT sensor which is the more conventional method. We have also shown that pressing a ceramic paste could lead to strong anisotropic shrinkage. For instance, the overall shrinkage of kaolin in the pressing direction is 1.8 times greater than in the other

directions, while for alumina it is significantly less. The anisotropic shrinkage is related to the morphology of grains inducing a larger water/solid ratio along one direction compared to the two other orthogonal directions.

In ceramic processing, taking into account the shrinkage of green bodies during drying is of strong importance to ensure dimensional accuracy. Furthermore, an optical approach has potential for incorporation into industrial production lines with eventual corrective action.

Acknowledgments

Siham Oummadi thanks the Nouvelle-Aquitaine Region for financial support of her Ph.D.

References

- [1] Scherer GW. Theory of Drying. *Journal of the American Ceramic Society*. 1990;73(1):3–14.
- [2] Brosnan DA, Robinson GC. *Introduction to Drying of Ceramics: With Laboratory Exercises*. 1st ed. Book Published by The American Ceramic Society; 2003.
- [3] Ford RW. *Ceramics Drying*. Pergamon Press; 1986.
- [4] Bigot A. Retrait au séchage des kaolins et des argiles. *Comptes rendus de l'Académie des Sciences*. 1921 Mar;p. 755–758.
- [5] Munier P, Gérard-Hirne J. La représentation graphique de la relation entre le retrait et l'humidité au cours du séchage des pâtes céramiques. *Bulletin de la Société Française de Céramique*. 1954;(25):3–10.
- [6] Kingery WD, Francel J. Fundamental Study of Clay: XIII, Drying Behavior and Plastic Properties. *Journal of the American Ceramic Society*. 1954;37(12):596–602.
- [7] Kornmann M. Complementary explanation of the Bigot' curve. *Industrie Céramique et Verrière*. 2006 Mar;p. 44–53.

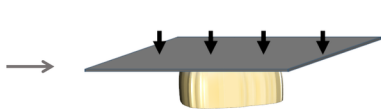
- [8] Mancuhan E, Özen S, Sayan P, Sargut S. Experimental investigation of green brick shrinkage behavior with Bigot's curves. *Drying Technology*. 2016 Oct;34:1535–1545.
- [9] Manuel Miguel J, Pardo Fabregat F, Montero MA. Ceramic behaviour of clays in Central Chile. *Applied Clay Science*. 2018 Jun;157.
- [10] Miranda S, Patruno L, Ricci M, Saponelli R, Ubertini F. Ceramic sanitary wares: Prediction of the deformed shape after the production process. *Journal of Materials Processing Technology*. 2015 Jan;215:309–319.
- [11] Tari G, Ferreira J, Fonseca A. Influence of Particle Size and Particle Size Distribution on Drying-Shrinkage Behavior of Alumina Slip Cast Bodies. *Ceramics International*. 1999 Aug;25:577–580.
- [12] Bretagne N, Valle V, Dupré JC. Development of the marks tracking technique for strain field and volume variation measurements. *NDT and E International*. 2005;4(38):290–298.
- [13] Tang CS, Shi B, Liu C, Suo WB, Gao L. Experimental characterization of shrinkage and desiccation cracking in thin clay layer. *Applied Clay Science*. 2011 Apr;52(1):69–77.
- [14] Yilmaztürk F, Kulur S, Pekmezci B. Measurement of shrinkage in concrete samples by using digital photogrammetric methods. *The International Archives of the Photogrammetry, Remote Sensing and Spatial Information Sciences*. 2004 Jan;34.
- [15] Onoda GY. Specific Volume Diagrams for Ceramic Processing. *Journal of the American Ceramic Society*. 1983;66(4):297–301.
- [16] Monk M, Lee H, Carty WM. Determining the Water Content for Castable Slump Using Specific Volume Diagram Approach. *Proc of the 54th Annual Symposium on Refractories, St Louis, MO, American Ceramic Society*. 2018;.
- [17] Oummadi S, Nait-Ali B, Alzina A, Victor JL, Launay Y, Mirdrikvand M, et al. Distribution of water in ceramic green bodies during drying. *Journal of the European Ceramic Society*. 2019;39(10):3164–3172.

- [18] Belrhiti Y, Gallet-Doncieux A, Germaneau A, Doumalin P, Dupre JC, Alzina A, et al. Application of optical methods to investigate the non-linear asymmetric behavior of ceramics exhibiting large strain to rupture by four-points bending test. 2012;32(16):4073–4081.
- [19] Grédiac M. The use of heterogeneous strain fields for the characterization of composite materials. 1996;56(7):841–846.

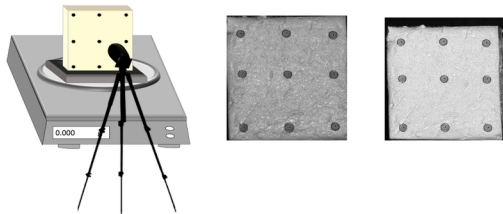
(1) Ceramic paste



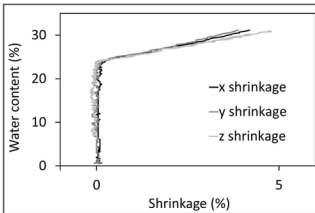
(2) Pressing



(3) Tracking of marks & monitoring mass

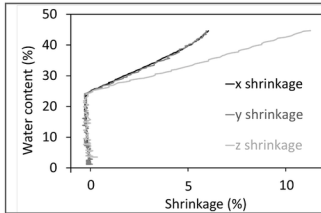


(4) Plot of Bigot curves in different directions



Alumina paste:

almost isotropic shrinkage



Kaolin paste:

orientation of platelets

↓
strong anisotropic shrinkage